

169
171

HEAVY ION RADIATION DAMAGE ANNEALING IN GARNET CRYSTAL

SURINDER SINGH, LAKHWANT SINGH, JASPAL SINGH and H.S. VIRK

Department of Physics, Guru Nanak Dev University,
Amritsar-143005, India

ABSTRACT

The annealing kinetics of U-238 (15.36 MeV/n) ion produced defects in garnet as a function of both time and temperature are investigated. Two annealing processes one at lower temperature range and the other at higher temperature range are found and described by two empirical relations, based on the extensive experimental annealing data. It is observed that the track etch velocity parameter is more sensitive at lower temperatures while at higher temperatures the track retention rate dominates for the annealing studies. The values of two activation energies corresponding to two annealing stages are determined using empirical relations.

INTRODUCTION:

Energetic heavy ions penetrating through the crystalline minerals, create a linear damage (latent track) along their trajectory and leave behind much physics related to the damaged and undamaged material to be investigated. Latent tracks involve the different atomic and nuclear processes, producing various types of defects. Each type of defect can be associated with a different interaction process between incident ion and target material. To investigate such defects, Dartyge *et al.* (1981) carried out small angle X-ray scattering experiments on four silicates (viz: muscovite mica, labradorite, pyroxen and olivine) pre-irradiated with Ne, Ar, Fe, Cu, Kr and Xe ions. On the other hand, Albrecht *et al.* (1985) employed an independent series of the experiments to investigate the heavy ion produced defects in various dielectrics. However, authors of both the papers (Dartyge *et al.*, 1981; Albrecht *et al.*, 1985) have not tried to interpret the defect studies from microscopic etching and annealing experiments. Moreover, most of the previous annealing studies have been carried out on the undefined fission fragment tracks in crystalline minerals, glasses and plastics. It is obvious that these studies do not reveal the reaction kinetics to predict the annealing behaviour for arbitrary initial damage. However, the related studies (Ritter and Mark, 1984) have been attempted to elucidate the contribution of various reaction mechanisms, but still the existing theories are being questioned to understand the complete annealing mechanism (Singh and Singh, 1989; Singh *et al.*, 1990).

In the present paper an attempt has been made to understand the annealing mechanism of U-238 (15.36 MeV/n) ion latent tracks incident at {110} plane of garnet crystal.

TRACK ITSELF AND ITS ANNEALING MECHANISM

It is assumed that the main part of the heavy ion energy is imparted to ionize the atoms along its trajectory (Fleischer *et al.*, 1975) and produced ionic defects. Some part of heavy ion energy is used to displace the atoms from their normal lattice sites to interstitial positions and create interstitial-vacancy pairs. Both types of defects are known as point defects. The main type of the defects which play a vital role in the formation of etchable heavy ion trails are known as the extended defects. These defects involve the coulombic repulsive forces as well as the relaxation of the elastic and mechanical stresses and strains between ionic defects and bulk of the solid. So it is proposed that heavy ion latent track consists of all the above types of defects, particularly of extended defects, which are separated from the zones of loaded point defects.

It is believed that these defects diffuse to defect sinks to heal the damage, particularly when the exposed samples are subjected to thermal treatment. To understand the systematic annealing mechanism, the different isothermal and isochronal annealing experiments are performed on the U-238 (15.36 MeV/n) ion tracks incident at {110} plane of garnet crystal.

Before discussing the present investigations, It is required to give here some previous work regarding the annealing behaviour of radiation damage due to electrons and α -particles in crystals.

Fletcher and Brown (1953) proposed three annealing stages of the defects produced by electrons in crystal lattice on the basis of electrical parameters. On the other hand Stout *et al.* (1988) conducted isothermal and isochronal annealing experiments on the α -decay damage in natural UO_2 and ThO_2 . They found that the damage can be recovered by two annealing stages which correspond to lower and higher temperature ranges.

In the present studies, we have not only found two recovery stages of the heavy ion damage but also checked the two recently proposed empirical formulations, which describe the annealing mechanism in case of U-238 (15.36 MeV/n) ion tracks in garnet crystal.

In our simple microscopic etching and annealing experiments, since we have two measureable physical parameters i.e. the track etch rate V_T and track retention rate r , as a function of annealing time and temperature. We can relate these parameters with the activation energy for annealing. The first empirical relation is given by :

$$\frac{V_T(0) - V_T(t)}{t} = A t^{-n} \exp(-E_{eff}/KT) \quad (1)$$

where $V_T(0)$ and $V_T(t)$ are the etching rates, before and after annealing, K , the Boltzmann's constant, n , the exponent of annealing time and E_{eff} , is the effective activation energy for monomolecular recombination of point defects. The etching rates used here are the instantaneous etching rates and are determined from the slope of the linear portion of the curves (Fig.1).

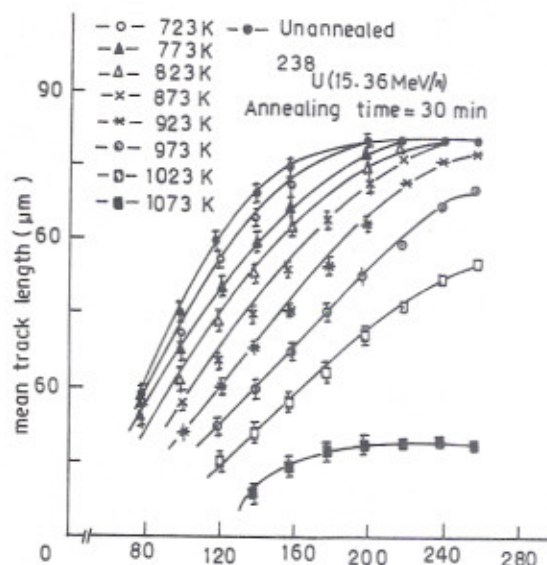


Fig.1. Plot of mean track length vs etching time of unannealed and annealed tracks at different annealing temperatures for constant annealing time (30 min)

It is verified that the experimental data involving the etching rates of annealed and unannealed tracks is found to be the best fit in the above empirical relation only upto a temperature of 873 K, however, at higher temperatures, the fitting diminishes gradually. The decrease in etching rate at the initial annealing stage shows that the free energy deposited along the environs of the latent track goes on decreasing. It is further found that the etchable track length remains almost constant during this annealing stage (Fig.2). Thus this annealing stage can be termed as the stage of

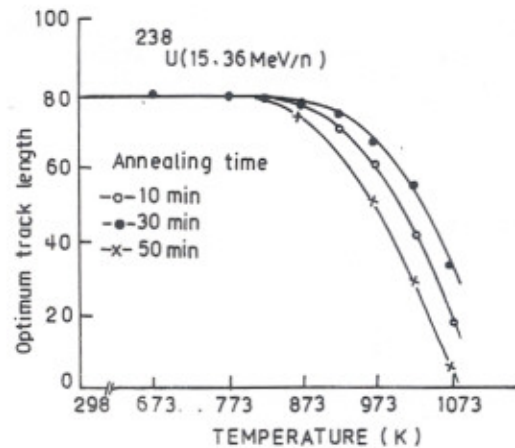


Fig. 2. Plot of optimum track length vs annealing temperature for varying annealing time (10-50 minutes).

monomolecular recombination of the point defects. For calculating the effective activation energy for this stage eq.1 can be rewritten as :

$$\ln \frac{V_T(0) - V_T(t)}{t} = \ln A - n \ln t - \frac{E_{\text{eff}}}{KT} \quad (2)$$

The slope of the graph (Fig.3) between left hand side of eq.2 and T^{-1} will give the effective activation energy for monomolecular recombination of point defects.

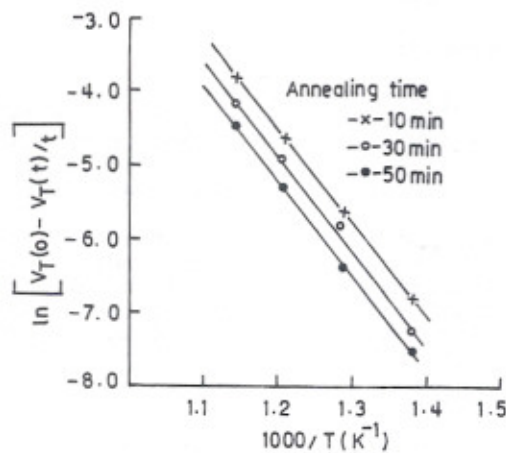


Fig. 3. The plot of $\ln[(V_T(0)-V_T(t))/t]$ vs T^{-1} for different annealing times, which gives the activation energy for recombination of point defects at lower range of annealing temperature.

When the experiments are carried out at higher temperatures, the experimental data relating the etching rates as a function of time and temperature could not be described by eq.1. However, at the same time, the experimental data involving other physical parameter i.e. the track retention rate r , plays a predominant role over annealing. It may be due to the healing of extended defects and consequently involves the second annealing stage, which can be described by the following empirical relation:

$$1-r = A t^{1-n} \exp(-Q/KT) \quad (3)$$

where $r = l(t)/l(0)$, is the ratio of the annealed and unannealed track length and is known as track retention rate. A is the annealing constant depending upon the nature of the ion and target material. To determine the activation energy for this stage, the above eq. can be rewritten as :

$$\ln(1-r) = \ln A + (1-n) \ln t - Q/KT \quad (4)$$

The slope of the curves (Fig.4) between $\ln(1-r)$ and T^{-1} will give the activation energy for the second annealing stage.

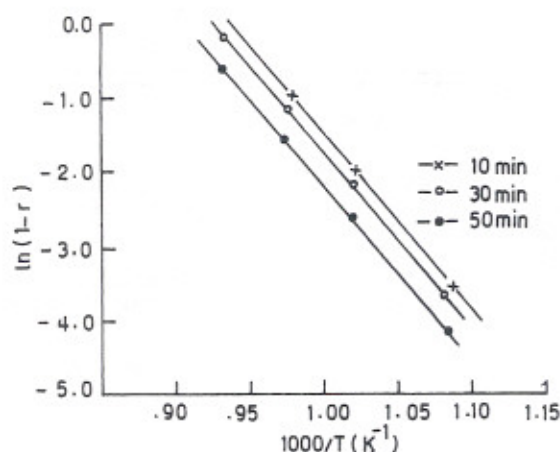


Fig. 4. The plot of $\ln(1-r)$ vs T^{-1} for different annealing times which gives the activation energy for transient diffusion of atoms towards the defect sinks at higher range of temperatures.

EXPERIMENTAL PROCEDURE:

Samples of $\{1\bar{1}0\}$ plane of garnet crystal are prepared by cutting, grinding and polishing. Cerium oxide was used as a polishing material. A final lap of polishing was given using diamond paste of different grades (8 μ m, 6 μ m and 2 μ m). The samples were then irradiated with U-238 (15.36 MeV/n) ions incident at 30° from UNILAC heavy ion accelerator at GSI, Darmstadt, Germany.

The irradiated samples were cut into a large number of small samples (2mm X 2mm) for isothermal and isochronal annealing studies. Experiments were performed in the temperature controlled muffle furnace ($\pm 3^\circ$ C accuracy). The samples were etched in 15N-KOH boiling solution for different etching times. The etched samples were washed, dried and scanned under Carl-Zeiss binocular microscope for measuring the track parameters.

RESULTS AND DISCUSSION

Fig. 1 shows the variation of mean track length with etching time of unannealed and annealed tracks of U-238 (15.36 MeV/n) in $\{1\bar{1}0\}$ plane of garnet crystal. The upper most curve represents the data for reference sample while all other curves belong to the data of annealed tracks for constant annealing time (30 min) at eight different temperatures (723, 773, 823, 873, 923, 973, 1023 and 1073 K). It can be observed from these curves that there

is a linear increase in track length in the beginning and then smoothen off, which indicates that the full track length has been revealed and becomes independent of the etching time.

Fig. 3 shows that there is no change in the optimum track length up to certain annealing temperature (873 K). However, at the same time there occurs a regular decrease in track etch rate, which can be attributed to the annealing of point defects. At this stage the monomolecular recombination of the ionic defects and interstitial-vacancy pairs has taken place and the annealing data is described by eq.1. When the experiments are carried out at higher temperature range (923-1073 K), then the annealing data involving the change in track etch rate, failed to be described by eq.1. However, at the same time, the other parameter i.e. the track retention rate plays a

Table 1. The values of track etch velocity V_T and track reduction rate r , of U-238 (15.35 MeV/n) ion track incident at 30° in the $\{1\bar{1}0\}$ plane of garnet crystal for constant time (30 min) and different annealing temperatures.

Annealing temp. (K)	Track etch rate, V_T ($\mu\text{m}/\text{min}$)	$\ln \frac{V_T(0)-V_T(t)}{t}$	Track retention rate, r	$\ln(1-r)$
*				
298	0.820	-	-	-
723	0.795	-7.26	-	-
773	0.735	-5.86	-	-
823	0.602	-4.92	0.99	-4.60
873	0.378	-4.21	0.98	-3.91
923	0.352	-4.16	0.97	-3.61
973	0.331	-4.11	0.12	-2.15
1023	0.280	-4.01	0.32	-1.25
1073	0.220	-3.91	0.22	-0.25

* Unannealed

predominant role to study the systematic annealing behaviour. Thus there is another annealing process at higher temperature range. At this stage the annealing of extended defects along with that of point defects occurs, which can be interpreted as transient diffusion of the recombined atoms towards the defect sinks. This annealing phenomenon is similar to as proposed by (Fletcher and Brown, 1953) and can be mathematically described by eq.3. The experimental annealing data at low and higher temperature ranges, involving the variation of track etch rate and track length retention rate is given in the Table 1. The activation energy for annealing of point defects or the first annealing stage is calculated from the slope of graph (Fig.3) using eq.2. The activation energy for the second annealing stage is calculated from the slope of the graph (Fig.4) using eq.4. The values of the activation energies

Table. 2. The values of activation energies for two annealing stages of U-238 (15.36 MeV/n) ion tracks in $\{1\bar{1}0\}$ plane of garnet crystal for different annealing times.

Ion (Energy)	Annealing Time (min)	Activation energy (eV)	
		1st stage (E_{eff})	2nd stage (Q)
U-238 (15.36 MeV/n)	10	1.09	2.02
	30	1.08	1.98
	50	1.07	2.01

of both the annealing stages for varying annealing times (10-50 min.) are given in Table 2. It can be noted that the activation energy for each annealing stage is independent of the annealing time.

ACKNOWLEDGEMENT

The financial assistance rendered by Council of Scientific and Industrial Research (CSIR) in the form of Senior Research Fellowship is gratefully acknowledged. Thanks are due to Drs. J.Vetter and R.Spohr for providing the irradiation facility at GSI Darmstadt. We are thankful to Mr.Santokh Singh for neatly drawing the figures.

REFERENCES

- Albrecht, D., P. Armbruster and R. Spohr (1985). Investigation of heavy ion produced defect structures in insulators by small angle scattering. Appl. Phys. **A37**, 37.
- Dartyge, E., J.P. Duraud, Y.Lengevin and M. Maurette (1981) New model of nuclear particle tracks in dielectric minerals. Phys. Rev., **B23** 5213.
- Fleischer, R.L., P.B. Price and R.M. Walker (1975) Nuclear tracks in solids. University of California, Berkeley.
- Fletcher, R.C. and W.L. Brown (1953). Annealing of bombardment damage in a diamond-type lattice. Phys. Rev. **92**, 585
- Ritter, W. and T.D. Mark (1984). Optical studies of radiation damage and its annealing in natural fluorapatite. Nucl. Instr. Meth. **B1**, 394.
- Singh, L. and S. Singh (1989). Annealing kinetics of heavy ion produced defects in crystalline minerals. Nucl. Instr. Meth. **B44**, 90.
- Singh, L., A.S. Sandhu, S. Singh and H.S. Virk (1989). Thermal annealing of heavy ion tracks in muscovite mica. Rad Eff. and Def. in solids. **108**, 257.
- Stout P.J., G.R. Lumpkin, R.C. Ewing and Y. Eyal (1988). An annealing study of alpha-decay damage in natural UO₂ and ThO₂. Mat. Res. Soc. Symp. Proc. **112**, 495.